THE EUROPEAN
PHYSICAL JOURNAL C

Regular Article - Theoretical Physics

Near-threshold photoproduction of J/ψ in two-gluon exchange model

Fancong Zeng[1], **Xiao-Yun Wang**[1,2,a], **Li Zhang**[1,2], **Ya-Ping Xie**[3,4,b], **Rong Wang**[3,4,c], **Xurong Chen**[3,4,5,d]

[1] Lanzhou University of Technology, Lanzhou 730050, China
[2] Department of Physics, Lanzhou University of Technology, Lanzhou 730050, China
[3] Institute of Modern Physics, Chinese Academy of Sciences, Lanzhou 730000, China
[4] University of Chinese Academy of Sciences, Beijing 100049, China
[5] Guangdong Provincial Key Laboratory of Nuclear Science, Institute of Quantum Matter, South China Normal University, Guangzhou 510006, China

Abstract The near-threshold photoproduction of J/ψ is regarded as one golden process to unveil the nucleon mass structure, pentaquark state involving the charm quarks, and the poorly constrained gluon distribution of the nucleon at large x (> 0.1). In this paper, we present an analysis of the current experimental data under a two-gluon exchange model, which shows a good consistency. Using a parameterized function form with three free parameters, we have determined the nucleonic gluon distribution at the J/ψ mass scale. Moreover, we predict the differential cross-section of the electroproduction of J/ψ as a function of the invariant mass of the final hadrons W, at EicC, as a practical application of the model and the obtained gluon distribution. According to our estimation, hundreds of J/ψ events can be detected per year on EicC near the threshold. Therefore, the relevant experimental measurements are suggested to be carried out on EicC.

1 Introduction

The photoproduction of J/ψ close to the threshold is a key experimental channel widely discussed to investigate the pentaquark photoproduction, for the charm production near the threshold has a strong sensitivity to the multi-quark, the gluonic and the hidden-color correlations to the hadronic and nuclear wavefunctions in QCD [1]. Moreover, the near-threshold photoproduction of J/ψ also plays an important role in probing the nucleon mass structure [2–8], as has been

recently illustrated with a very preliminary analysis [9] of the GlueX data [10]. On the experimental side, there has been some progresses reported and undergoing [10–13].

Recently, the first measurement of the near-threshold cross-section of the reaction $\gamma p \rightarrow J/\psi p$ has been reported [11]. Including the GlueX data, the photon-gluon fusion model and the pomeron exchange model [14] has been demonstrated to be applicable to explain the heavy quarkonia photoproduction in a wide energy range. More sophisticated models based on the three-gluon exchange, the holographic QCD, and the dispersion relation are developed [15–19], and taken to explain the recent data. Unfortunately, it is difficult for these models to give the differential cross-section at the production threshold, where some variations of the predictions are found. There are many models that can describe the photoproduction of $\gamma p \rightarrow J/\psi p$ successfully in different energy ranges. Among them, the two-gluon exchange model captures our attention. One work [15] shows the total and differential cross-sections compared with the experimental data, providing some ideas and literatures for us to do this work, confronting with the recent experimental data. The exclusive photoproductions of all vector mesons by real and virtual photons are studied in a soft dipole Pomeron model [20], which has a perfect quality of fitting to both the total and the differential cross-sections in the high energy region. However, there is an inconsistency for the differential cross-section near the threshold. In a related work [21], the contribution of pentaquark state P_c was added, which is based on the nonresonant contribution parametrized with the soft dipole Pomeron model.
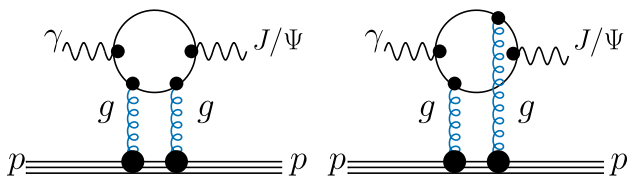
The total elastic $J/\psi - p$ production at high photon-nucleon invariant mass W is well described by the $t-$channel exchange of a colorless object between the photon and the proton [22]. In this paper, two-gluon exchange model is

[a] e-mail: xywang@lut.edu.cn (corresponding author)

[b] e-mail: xieyaping@impcas.ac.cn

[c] e-mail: rwang@impcas.ac.cn

[d] e-mail: xchen@impcas.ac.cn

Fig. 1 The schematic Feynman diagram of the two-gluon exchange model for J/ψ production

applied to fit the data by GlueX Collaboration [10]. This makes the total and differential cross-sections depend on the gluon distribution function squared, while the conventional gluon distribution function from GRV98 [23], NNPDF [24], CJ15 [25,26], and IMParton16 [27] are difficult to interpret the new GlueX data [10], within the framework of the two-gluon exchange model. Thus we plan to use a simplified gluon distribution parametrization [28] that has the form $xg\left(x, m_J^2\right) = A_0 x^{A_1}(1 - x)^{A_2}$ to perform a fit to the near-threshold J/ψ photoproduction data. The other purpose of this work is to predict the total and differential cross-sections of J/ψ electroproduction at different energies near the threshold, based on the obtained gluon distribution, in order to remove some model uncertainties from the gluon distribution. Nowadays, the high and low energy Electron Ion Colliders (EIC) are vigorously proposed to be built for probing the deepest structure inside hadron, which is the main building block of the visible universe. US EIC is on the way and focus on the high energy collisions [29], and the opportunities of Chinese EIC are now under some hot discussions [30,31]. To make predictions for the future machines are necessary.

The paper is organized as follows. The formulas of the two-gluon exchange model and the J/ψ production via electron-proton collisions are provided in Sect. 2. Then in Sect. 3, we show the numerical result on the explanations of the current experimental data, the extracted gluon distribution, and the predictions of J/ψ production on EicC [30,31]. A short summary is given in Sect. 4.

2 Formalism

The two-gluon exchange model is based on the photon fluctuation into the quark-antiquark pair ($\gamma \rightarrow q + \bar{q}$) and the picture of the double gluon exchange between the nucleon state and the quark-antiquark pair, which is illustrated in Fig. 1. In the process as shown in Fig. 1, the photon splits into a dipole with c and $\bar{c}$ at first. Then, the dipole scatters off the initial proton by exchanging two-gluon. Finally, the dipole forms into final state J/ψ and initial proton keeps interact proton since two gluons are colorless. Because the valence quark of proton is u and d quark, the process exchanging two valence quarks can be neglected in J/ψ production process.

In a word, the two-gluon exchanging process is dominant in J/ψ production near threshold.

Due to the hard scale in the heavy quarkonium production, the exclusive vector meson photoproduction amplitude is factorized as a reasonable assumption. In a lowest order perturbative QCD of factorization, the photoproduction of J/ψ amplitude is given by [32–34],

$$\mathscr{T} = \frac{i2\sqrt{2}\pi^2}{3}m_q\alpha_s e_q f_V F_{2g}(t)$$
$$\int dl^2 D_g^2(l)\left[D_+(l) - D_-(l)\right]G(l). \qquad (1)$$

where $m_q = 1.27$ GeV is the mass of the quark, e_q is the charge of the quark. The meson decay constant f_V is deduced from the leptonic decay width, which is given by [35],

$$\Gamma_{e^+e^-} = \frac{4\pi\alpha^2}{3m_J}f_V^2. \qquad (2)$$

By taking the radiative decay width $\Gamma_{e^+e^-} = 5.547$ keV from PDG average [36], the electromagnetic coupling constant $\alpha = 1/137$, yield $f_V = 0.278$ GeV.

The gluon propagator $D_g(l)$ in Eq. (1) is taken to be $1/l^2$. $D_-(l)$ represents the propagator of the off-shell quark when the two gluons couple to different quarks of the vector meson, which is written as,

$$D_-(l) = \left(-2m_q^2 - 2l^2\right)^{-1}, \qquad (3)$$

while $D_+(l)$ represents the propagator of the off-shell quark when the two gluons couple to the same quark in the vector meson, which is written as,

$$D_+(l) = \left(-2m_q^2\right)^{-1}. \qquad (4)$$

The factor $F_{2g}(t)$ in Eq. (1) accounts for the dependence of the amplitude with respect to the two gluon correlation in the proton, and it is written as [32,37],

$$F_{2g}(t) = \frac{4m_p^2 - 2.8t}{4m_p^2 - t}\frac{1}{(1 - t/t_0)^2}, \qquad (5)$$

in which $t_0 = 0.71$ GeV^2 and m_p is the proton mass. $G(l)$ defines the probability for the dipole to catch the gluon of momentum l from the proton. Its integral is related to the gluon distribution function $xg(x)$, which is written as [32, 33],

$$xg\left(x, Q^2\right) = \int dl^2 \frac{G(l)}{l^2}. \qquad (6)$$

With the above discussions, the two-gluon exchange amplitude becomes [37],

$$
\mathcal{T} = \frac{i\sqrt{2}\pi^2}{3} m_q \alpha_s e_q f_V F_{2g}(t) \left[\frac{xg\left(x, Q_0^2\right)}{m_q^4} \right.
$$
$$
\left. + \int_{Q_0^2}^{+\infty} \frac{dl^2}{m_q^2 \left(m_q^2 + l^2\right)} \frac{\partial xg\left(x, l^2\right)}{\partial l^2} \right]. \tag{7}
$$

The amplitude is normalized and $\frac{d\sigma}{dt} = \alpha |\mathcal{T}|^2$. In the lowest order, the J/ψ photoproduction differential cross-section is given as [37],

$$
\frac{d\sigma}{dt} = \frac{\pi^3 \Gamma_{e^+e^-} \alpha_s}{6\alpha m_q^5} \left[xg\left(x, m_J^2\right) \right]^2 \exp(bt), \tag{8}
$$

where $x = m_J^2/W^2$, α_s is the QCD coupling constant [14]. The exponential slope b of t-dependence is found to be $1.67 \pm 0.38 \,\text{GeV}^{-2}$ at $W = 4.59 \,\text{GeV}$ [10]. Here, the W-dependence of the slope b can be evaluated with an empirical formula as $b = \frac{d}{dt} \ln\left[\frac{d\sigma}{dt}\right]$.

The $xg\left(x, m_J^2\right)$ is the gluon distribution function at $Q^2 = m_J^2$, and in this work it is parameterized using a simple function form $xg\left(x, m_J^2\right) = A_0 x^{A_1} (1-x)^{A_2}$ [28]. Fixing the gluon parametrization is one of our purposes in this work. The poles at $x = 0$ and $x = 1$ in the parametrization are the singularities associated with Regge behavior at small x and the quark counting rules at large x. The parameters A_0, A_1, A_2 can be fixed by the experimental data.

The total cross-section is obtained by integrating the differential cross-section (Eq. 8) over the allowed kinematical range from $|t_0|$ to $|t_1|$, here, $t_0(t_1) = \left[\frac{m_1^2 - m_3^2 - m_2^2 + m_4^2}{2W}\right]^2 - (p_{1cm} \mp p_{3cm})^2$, $p_{icm} = \sqrt{E_{icm}^2 - m_i^2}(i = 1, 3)$, $E_{1cm} = \frac{W^2 + m_1^2 - m_2^2}{2W}$, $E_{3cm} = \frac{W^2 + m_3^2 - m_4^2}{2W}$ [38] and $W = 4.59$ GeV. Therefore, the total cross-section can be written as,

$$
\sigma = \frac{0.487}{b(W)} \frac{\pi^3 \Gamma_{e^+e^-} \alpha_s}{6\alpha m_q^5} \left[xg\left(x, m_J^2\right) \right]^2. \tag{9}
$$

The exponential slope $b(W)$ has little vary with the energy W [12,39–41]. Studies of S. Chekanov imply that the b function in the high energy region could be formulated as [39],

$$
b(W) = b_0 + 0.46 \cdot In(W/W_0). \tag{10}
$$

In order to estimate $b(W)$ in the low energy region near threshold, we fixed the slope to be the measured value $1.67 \pm 0.38 \,\text{GeV}^{-2}$ at the energy $W_0 \simeq 4.59^{+0.21}_{-0.15} \,\text{GeV}$ [10]. In Fig. 2, it is obvious to see that b has a weak W-dependence in a wide energy range. It is precisely because the value of b changes very slowly with energy that even after we consider
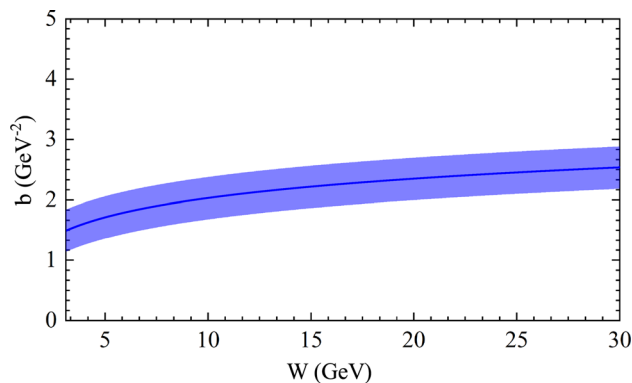
Fig. 2 The exponential slope b as a function of the energy W. Here, the band stand for the error bar of the b

the error of b, the value of b is still between $1\sim2 \,\text{GeV}^{-2}$ near the energy threshold. Therefore, we roughly think that the uncertainty of the b has little effect on the numerical results of the cross-section for the J/ψ photoproduction.

The exclusive electroproduction of J/ψ is closely connected J/ψ photoproduction, as in the electron scattering process the J/ψ vector meson is generated from the virtual photon exchanged between the electron and the hadron. The electroproduction cross-section of J/ψ in electron-proton scattering can be found in the recent literatures [42,43],

$$
\sigma(ep \to eJ/\psi p)
$$
$$
= \int dk dQ^2 \frac{dN^2(k, Q^2)}{dk dQ^2} \sigma_{\gamma^* p \to J/\psi p}(W, Q^2), \tag{11}
$$

here W is the center-of-mass energy of the photon-proton system, k is the momentum of the virtual photon emitted from the electron beam in the target rest frame, and Q^2 is the virtuality of the photon. The photon flux is given as [44],

$$
\frac{d^2 N(k, Q^2)}{dk dQ^2} = \frac{\alpha}{\pi k Q^2} \left[1 - \frac{k}{E_e} + \frac{k^2}{2E_e^2} - \left(1 - \frac{k}{E_e}\right) \left| \frac{Q_{min}^2}{Q^2} \right| \right], \tag{12}
$$

where E_e is the energy of the initial electron in proton rest frame, and Q_{min}^2 is given as,

$$
Q_{min}^2 = \frac{m_e^2 k^2}{E_e(E_e - k)}. \tag{13}
$$

The maximum Q^2 is determined by the energy loss of the initial electron,

$$
Q_{max}^2 = 4E_e(E_e - k). \tag{14}
$$

The connection between the cross-section induced by a real photon and that induced by a virtual photon is governed by,

Table 1 The fitted values of the parameters A_0, A_1, A_2 describing the gluon distribution function $xg(x)$ and the reduced χ^2/d.o.f. in the low W region

| A_0	A_1	A_2	χ^2/d.o.f.
0.71 ± 0.12	-0.00061 ± 0.00045	2.83 ± 0.26	0.20
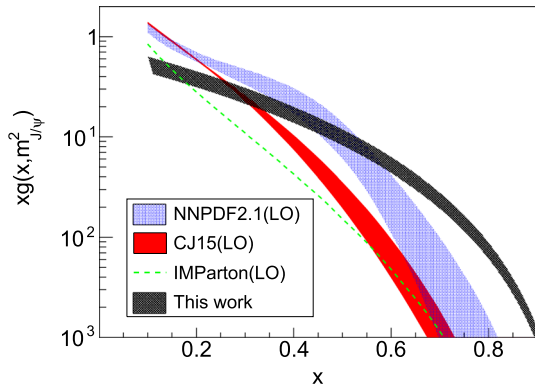
Fig. 3 The gluon distribution extracted from the near-threshold J/ψ photoproduction data under the two-gluon exchange model

$$\sigma_{\gamma^* p \to J/\psi p}(W, Q^2)$$
$$= \sigma_{\gamma p \to J/\psi p}(W, Q^2 = 0)\left(\frac{M_V^2}{M_V^2 + Q^2}\right)^{\eta}. \quad (15)$$

in which $\eta = c_1 + c_2(M_V^2 + Q^2)$ with the values of $c_1 = 2.36 \pm 0.20$ and $c_2 = 0.0029 \pm 0.43$ GeV^2 [42]. With the known photon flux from the electron beam and the photon virtuality dependence of the cross-section, we can calculate the total cross-section in electron-proton scattering near the production threshold.

3 Numerical results

The parametrization $xg(x, m_J^2) = A_0 x^{A_1}(1 - x)^{A_2}$ of the nucleon gluon distribution is introduced and used in the two-gluon exchange model discussed in the above section. The free parameters A_0, A_1, A_2 then are fixed by a global analysis of both the total cross-section data [10,39,45,46] and the near-threshold ($W = 4.59$ GeV) differential cross-section data by GlueX collaboration [10]. The obtained parameters are listed in Table 1. Figure 3 shows our obtained gluon distribution in this work, compared with the predictions from the widely used global fits, such as NNPDF [24], CJ15 [25,26] and IMParton [27]. It is found that the gluon distributions determined by different groups are more or less consistent with each other in the low x range of $x < 0.3$. On the other side, our obtained gluon distribution is higher than other predictions when $x > 0.6$.
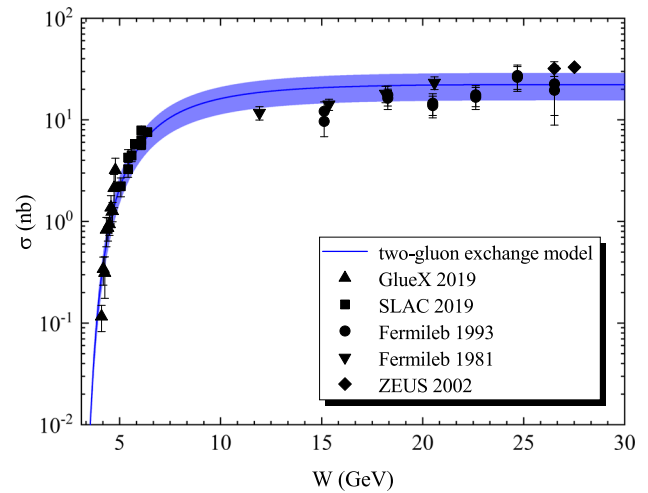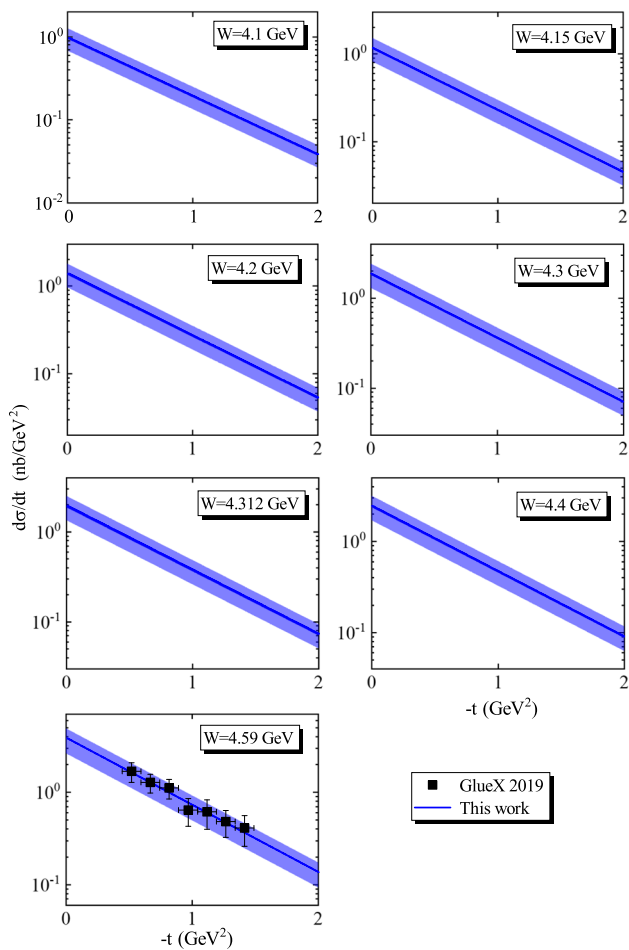

Fig. 4 The total cross-section of the channel $\gamma p \to J/\psi p$ as a function of W. Here, the band stand for the error bar of the A_0
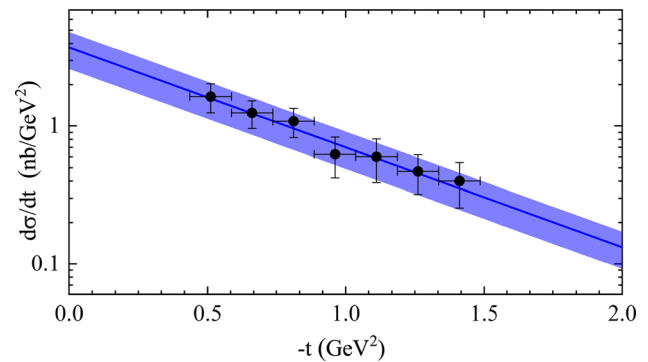
Fig. 5 The fitted differential cross-section as a function of four momentum transfer squared t at $W = 4.59$ GeV compared to the measured data by GlueX [10]. Here, the band stand for the error bar of the A_0

The predicted total cross-section of $\gamma p \to J/\psi p$ as a function of center-of-mass energy W is shown in Fig. 4, compared to the experimental data from several experiments. The comparison between the differential cross-section in the two-gluon exchange model with the assumed exponential slope and the experimental measurement of the differential cross-section is manifested in Fig.5, exhibiting an amazing agreement. The two-gluon exchange model is valid to describe the J/ψ photoproduction near the production threshold.

Since the main purpose of this paper is to search the underlying mechanism of J/ψ photoproduction near the production threshold, the χ^2/N of the global fit in the low energy range ($W < 6.4$ GeV) is calculated to be 0.20. The χ^2/N value less than one indicates that the two-gluon exchange model is applicable for the near-threshold photoproduction of J/ψ. Note that the errors of the experimental data from Fermilab 1981 [45], Fermilab 1993 [46] and ZEUS 2002 [39] are kind of big. Hence, more future precise measurements on the near-threshold J/ψ production are needed. The
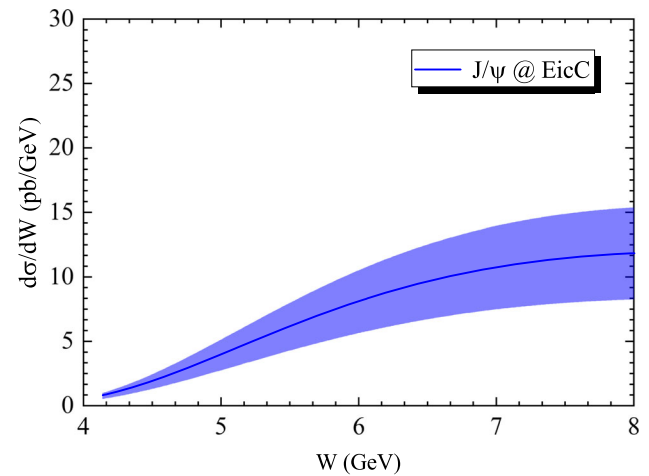
Fig. 6 The predicted differential cross-section as a function of four momentum transfer squared t at different W values. Here, the bands stand for the error bar of the A_0

Table 2 The values of $d\sigma/dt|_{t=0}$ at different values of energy W

W (GeV)	4.1	4.15	4.2	4.3	4.312	4.4	4.59
$d\sigma/dt|_{t=0}$	0.98	1.17	1.38	1.86	1.93	2.44	3.73
error	0.29	0.35	0.42	0.56	0.58	0.74	1.12

Fig. 7 The predictions of J/ψ electro-production cross-section as a function of W on EicC machine, with the selections of the low virtuality photons of 0.1 GeV$^2 < Q^2 < 1$ GeV^2. Here, the band stand for the error bar of the A_0

4 Summary

We have reproduced the total cross-section and the differential cross-section of the reaction $\gamma p \rightarrow J/\psi p$ near the production threshold with two-gluon exchange model encountering a parameterized gluon distribution function. The parameterized gluon distribution function is determined by a fit to the recent GlueX data, and it is found to be basically consistent with the global analyses of gluon distribution from other groups. An interesting finding is that in accordance with GlueX data and within the two-gluon exchange model, the gluon distribution does not go down quickly when x approaches one. Results inditate that two-gluon exchange model depicts well both the differential and the total cross-section of J/ψ in a wide energy range, and it can be used to predict the electroproduction cross-section near the production threshold. On EicC, the low energy EIC, the J/ψ production cross-section is around 10 pb based on our model, hence EicC will be an important and interesting future machine to collect the J/ψ data and to explore the exotic hadrons in the charm sector and the nucleonic mass structure. Assuming the integrated luminosity of EicC experiment can reach up to 50 fb^{-1} per year [30,31], taking the total cross-section $\sigma \simeq 0.7$ pb in the energy range 4.1 GeV $< W <$ 4.6 GeV, the total number of J/ψ produced on EicC then is 35000 ± 6000. Considering a detector efficiency of 20% and collecting both the decay di-electrons and the decay di-muons, we are going

J/ψ photoproductions near the threshold at more different energies are predicted by the two-gluon exchange model, which are shown in Fig. 6. The corresponding cross-sections at $t = 0$ GeV^2 are given in Table 2. These forward differential cross-sections are speculated to be connected to the nucleon mass.

The next generation of the advanced accelerator facility to study the J/ψ photoproduction is the electron-ion collider. The Electron ion collider in China (EicC) is under some hot discussions and proposed to be built and run at a low energy compared to the EIC in US. In order to investigate the opportunity of EicC in J/ψ study, we calculate the differential cross-section of J/ψ electroproduction as a function of the c.m. energy of the system of the emitted virtual photon and the proton, which is depicted in Fig. 7. The cross-section is around a doze of pb, which suggests a high yield rate at the high luminosity EicC.

to have about 800 ± 100 J/ψ near-threshold events detected per year. Thus, the precision of the near-threshold J/ψ production experiment on EicC is promising.

Data Availability Statement This manuscript has no associated data or the data will not be deposited. [Authors' comment: Since our work is to fit the experimental data with a physical model, the experimental data used are all published in the relevant literature. We only have the theoretical results of the fitting and cannot provide new experimental data.]

References

1. S.J. Brodsky, E. Chudakov, P. Hoyer, J.M. Laget, Phys. Lett. B **498**, 23–28 (2001). arXiv:hep-ph/0010343
2. X.D. Ji, Phys. Rev. Lett. **74**, 1071–1074 (1995). arXiv:hep-ph/9410274
3. X.D. Ji, Phys. Rev. D **52**, 271–281 (1995). arXiv:hep-ph/9502213
4. C. Lorcé, Eur. Phys. J. C **78**(2), 120 (2018). arXiv:1706.05853
5. D. Kharzeev, Proc. Int. Sch. Phys. Fermi **130**, 105–131 (1996). arXiv:hep-ph/9601029
6. D. Kharzeev, H. Satz, A. Syamtomov, G. Zinovjev, Eur. Phys. J. C **9**, 459–462 (1999). arXiv:hep-ph/9901375
7. S. Rodini, A. Metz, B. Pasquini, arXiv:2004.03704 [hep-ph]
8. A. Metz, B. Pasquini, S. Rodini, arXiv:2006.11171 [hep-ph]
9. R. Wang, J. Evslin, X. Chen, Eur. Phys. J. C **80**(6), 507 (2020). arXiv:1912.12040
10. A. Ali et al., GlueX. Phys. Rev. Lett. **123**(7), 072001 (2019). arXiv:1905.10811
11. E. Chudakov (GlueX Collaboration), https://agenda.infn.it/event/12464/contributions/14334/attachments/10583/11889/talk_spin_2018.pdf (2018)
12. Z.E. Meziani et al. arXiv:1609.00676
13. S. Joosten, Z.E. Meziani, PoS **QCDEV2017**, 017 (2018). arXiv:1802.02616
14. Y. Xu, Y. Xie, R. Wang, X. Chen, Eur. Phys. J. C **80**(3), 283 (2020). arXiv:2002.05340
15. Y. Hatta, D.L. Yang, Phys. Rev. D **98**(7), 074003 (2018). arXiv:1808.02163
16. Y. Hatta, A. Rajan, D.L. Yang, Phys. Rev. D **100**(1), 014032 (2019). arXiv:1906.00894
17. K.A. Mamo, I. Zahed, Phys. Rev. D **101**(8), 086003 (2020). arXiv:1910.04707
18. R. Boussarie, Y. Hatta, Phys. Rev. D **101**(11), 114004 (2020). arXiv:2004.12715
19. O. Gryniuk, S. Joosten, Z.E. Meziani, M. Vanderhaeghen, Phys. Rev. D **102**(1), 014016 (2020). arXiv:2005.09293
20. E. Martynov, E. Predazzi, A. Prokudin, Phys. Rev. D **67**, 074023 (2003). arXiv:hep-ph/0207272
21. X. Cao, J.P. Dai, Phys. Rev. D **100**(5), 054033 (2019). arXiv:1904.06015
22. L. Frankfurt, M. Strikman, Phys. Rev. D **66**, 031502 (2002). arXiv:hep-ph/0205223
23. M. Glück, E. Reya, A. Vogt, Eur. Phys. J. C **5**, 461–470 (1998). arXiv:hep-ph/9806404
24. R.D. Ball et al., NNPDF. Nucl. Phys. B **855**, 153–221 (2012). arXiv:1107.2652
25. J.F. Owens, A. Accardi, W. Melnitchouk, Phys. Rev. D **87**(9), 094012 (2013). arXiv:1212.1702
26. A. Accardi, L.T. Brady, W. Melnitchouk, J.F. Owens, N. Sato, Phys. Rev. D **93**(11), 114017 (2016). arXiv:1602.03154
27. R. Wang, X. Chen, Chin. Phys. C **41**(5), 053103 (2017). arXiv:1609.01831
28. J. Pumplin, D.R. Stump, J. Huston, H.L. Lai, P.M. Nadolsky, W.K. Tung, JHEP **07**, 012 (2002). arXiv:hep-ph/0201195
29. A. Accardi et al., Eur. Phys. J. A **52**(9), 268 (2016). arXiv:1212.1701
30. X. Chen, PoS **DIS2018**, 170 (2018). arXiv:1809.00448
31. X. Chen, PoS **SPIN2018** (2019), 160
32. M.G. Ryskin, Z. Phys. C **57**, 89–92 (1993)
33. S.J. Brodsky, L. Frankfurt, J.F. Gunion, A.H. Mueller, M. Strikman, Phys. Rev. D **50**, 3134–3144 (1994). arXiv:hep-ph/9402283
34. M.G. Ryskin, R.G. Roberts, A.D. Martin, E.M. Levin, Z. Phys, C **76**, 231–239 (1997). arXiv:hep-ph/9511228
35. O. Gryniuk, M. Vanderhaeghen, Phys. Rev. D **94**, 074001 (2016). arXiv:1608.08205
36. M. Tanabashi et al., [ParticleDataGroup],. Phys. Rev. D **98**, 030001 (2018)
37. A. Sibirtsev, S. Krewald, A.W. Thomas, J. Phys. G **30**, 1427–1444 (2004)
38. M.E. Peskin and D.V. Schroeder, *An Introduction to Quantum Field Theory* (Addison-Wesley,1995) 842
39. S. Chekanov et al., ZEUS. Eur. Phys. J. C **24**, 345–360 (2002). arXiv:hep-ph/0201043
40. C. Adloff *et al.* [H1], Phys. Lett. B **483**, 360-372 (2000). https://doi.org/10.1016/S0370-2693(00)00613-4. arXiv:hep-ex/0005010
41. A. Levy, Phys. Lett. B **424**, 191–194 (1998). https://doi.org/10.1016/S0370-2693(98)00160-9. arXiv:hep-ph/9712519
42. M. Lomnitz, S. Klein, Phys. Rev. C **99**(1), 015203 (2019). arXiv:1803.06420
43. S.R. Klein, Y.P. Xie, Phys. Rev. C **100**(2), 024620 (2019). arXiv:1903.02680
44. V.M. Budnev, I.F. Ginzburg, G.V. Meledin, V.G. Serbo, Phys. Rep. **15**, 181–281 (1975)
45. M.E. Binkley, C. Bohler, J. Butler, J.P. Cumalat, I. Gaines, M. Gormley, D. Harding, R.L. Loveless, J. Peoples, P. Callahan, G. Gladding, C. Olszewski, A. Wattenberg, Phys. Rev. Lett. **48**, 73 (1982)
46. P.L. Frabetti et al., Phys. Lett. B **316**, 197–206 (1993)